B-physics anomalies: The bridge between *R*-parity violating supersymmetry and flavored dark matter

Sokratis Trifinopoulos
Physik-Institut, Universität Zürich, CH-8057 Zürich, Switzerland

(Received 12 September 2019; published 10 December 2019)

In recent years, significant experimental indications that point toward lepton flavor universality violating effects in B-decays, involving $b \to c\tau\nu$ and $b \to s\ell^+\ell^-$, have been accumulated. A possible new physics explanation can be sought within the framework of R-parity violating supersymmetry, which contains the necessary ingredients to explain the anomalies via both leptoquark, tree-level exchange, and one-loop diagrams involving purely leptonic interactions. In addition, an approximate $U(2)^2$ flavor symmetry, that respects gauge coupling unification, successfully controls the strength of these interactions. Nevertheless, strong constraints from leptonic processes and Z boson decays exclude most of the relevant parameter space at the 2σ level. Moreover, R-parity violation deprives supersymmetry of its dark matter candidates. Motivated by these deficiencies, we introduce a new gauge singlet superfield, charged under the flavor symmetry and show that its third-generation, scalar component may participate in loop diagrams that alleviate the abovementioned tensions, while at the same time reproduce the observed relic abundance. We obtain a solution to both anomalies that is also fully consistent with the rich flavor and dark matter phenomenology. Finally, we assess the prospect to probe the model at future experiments.

DOI: 10.1103/PhysRevD.100.115022

I. INTRODUCTION

Testing the limits of the Standard Model (SM) by examining processes that might not respect lepton flavor universality (LFU) is one of the most prominent endeavors to discover new physics (NP) pursued at the LHC and several other experiments. Intriguingly, recent data exhibit anomalies in rare B-meson LFU violating decays, as encoded by the ratios,

$$R_{K^{(*)}} = \frac{\mathcal{B}(B \to K^{(*)}\mu\bar{\mu})}{\mathcal{B}(B \to K^{(*)}e\bar{e})}, \quad R_{D^{(*)}} = \frac{\mathcal{B}(B \to D^{(*)}\tau\bar{\nu})}{\mathcal{B}(B \to D^{(*)}\ell\bar{\nu})}, \quad (1)$$

which are almost free from theoretical uncertainties in hadronic matrix elements. $R_{D^{(*)}}$ concerns an enhancement of the charged-current interaction $b \to c\tau\nu$ [1–5] with respect to the tree-level induced SM amplitude [6,7], whereas $R_{K^{(*)}}$ a deficit in neutral-current transition involving $b \to s\ell^+\ell^-$ [8,9] at one-loop level [10]. They independently differ by approximately $3-4\sigma$ from their respective SM predictions and along with reported indications toward LFU violation in less theoretically clean observables, e.g., the angular observable P_5' in the $B \to K^*\mu\bar{\mu}$ decay [11–13] and the $R_{J/\Psi}$ ratio [14,15], constitute a consistent pattern of deviations that has motivated several attempts for a simultaneous explanation [16–60]. Nevertheless, the theoretical challenge to devise a UV complete model that accommodates all other low-energy observables has proven to be notoriously difficult and to the best of our knowledge, there have only been a handful of proposals in the bibliography so far [36,39,40,42,44,47,58].

Considering that the charged-current anomaly involves the tau and both of them the bottom, NP scenarios in which the third-generation SM fermions play a special role are favored. Furthermore, model-independent analyses suggest that $R_{K^{(*)}}$ can be resolved by singly modifying the Wilson coefficient (WC) of the semileptonic dimuon vector and axial operators, i.e., C_9^μ and C_{10}^μ [61–63]. In light of these observations, the potential of R-parity violating (RPV) supersymmetry (SUSY) to provide a comprehensive solution has been studied [52–59]. The minimal supersymmetric Standard Model (MSSM) particle content contains two third-generation, scalar particles, namely the right-handed sbottom $\tilde{b}_R$ and stau $\tilde{\tau}_R$, which in most models of spontaneous SUSY breaking are predicted to be significantly lighter than the first and second generations of superpartners at the electroweak scale [64]. If RPV interactions are turned on, $\tilde{b}_R$ has the right quantum numbers to mediate the required, large NP effects on $R_{D^{(*)}}$ at tree-level, while according to the novel result of [58], $\tilde{\tau}_R$ and $\tilde{b}_R$ can enter a box diagram, which generates a negative contribution to C_9^μ. Additionally, inspired by the corresponding

effective field theory (EFT) studies [18,22,31,32], it was shown that an approximate $U(2)^2$ flavor symmetry,[1] acting only on the first two generations, naturally suppresses the RPV couplings within the experimental bounds and still allows for an improvement over the SM fit. However, the possibility to completely alleviate the tensions in the ratios (1) and especially in $R_{K^{(*)}}$ is severely limited by the strict bounds on Z boson decay to leptons and tree-level, lepton flavor violating (LFV) τ decays.

The RPV setup preserves all the attractive features of SUSY, but one, namely the lightest supersymmetric particle (LSP) acting as dark matter (DM) candidate, because RPV interactions render it unstable. Therefore, we are compelled to speculate on the existence of new particles and the simplest, most popular example is that of a weakly interacting massive particle (WIMP),[2] which is thermally produced in the early Universe. Among the numerous WIMP models, those that assume a direct DM coupling to specific SM fermions and hence furnish distinctive collider signatures, are of particular interest. As with the case of RPV interactions, we would like to justify the apparent suppression of DM interactions with the first SM generation, which is most relevant to direct detection experiments. Consequently, we focus on the subclass of models, that explains from a flavor symmetry rationale the preference of DM to couple predominantly to particular flavors of either quark [67–79] or leptons [80–90], usually in minimal flavor violation (MFV)-type scenarios. Moreover, supersymmetric flavored DM models exhibit an even more restricted structure [71].

As long as the nature of DM remains a mystery, it is important to investigate any possible connection with other anomalous observations. To this end, there have been attempts to link mostly the $R_{K^{(*)}}$ discrepancy with DM [91–112]. In the current work, we address both anomalies in a supersymmetric framework related to a flavored hidden sector. The new particle content is economical, simply consisting of a gauge singlet, flavor multiplet and a $SU(2)_{\mathrm{L}}$ doublet, flavor singlet, chiral superfield, that acts as the mediator of a DM-lepton interaction. In analogy to the assumed MSSM mass spectrum, the third-generation scalar contained in the multiplet is taken to be the lightest component and thus the DM candidate. We revisit the $U(2)^2$ flavor symmetry that controls the strength of both DM and RPV interactions, so that it is compatible with grand unification theories (GUTs). By virtue of the spin and unsuppressed coupling of the DM particle to the τ_L, contributions are generated in one-loop diagrams involving purely leptonic interactions that interfere destructively with the ones generated by the RPV interactions. By exploring the interplay between the rich flavor and DM phenomenology, we determine whether it is possible to invoke an appropriate cancellation mechanism and at the same time reproduce the correct relic abundance for a natural choice of parameters. The performance of the overall fit is subsequently evaluated. Finally, we briefly discuss the implications for future experiments.

II. MODEL

A. R-parity violating interactions

Let us first review the R-parity odd and gauge-invariant superpotential, composed exclusively of MSSM quark and lepton superfields [113],

$$W_{\mathrm{RPV}} = \frac{1}{2}\lambda_{ijk} L_i L_j E^c_k + \lambda'_{ijk} L_i Q_j D^c_k + \frac{1}{2}\lambda''_{ijk} U^c_i U^c_j D^c_k, \quad (2)$$

where there is a summation over the flavor indices $i, j, k = 1, 2, 3$, and summation over gauge indices is understood.

The traditional motivation for R-parity is that it forbids the baryon-number breaking λ'' couplings and thus ensures proton stability, but this argument is no longer substantial. Notwithstanding, if the MSSM is an effective theory [114], higher-dimensional operators could also induce rapid proton decay and one should rely on different mechanisms, e.g., MFV-type flavor symmetries, to mitigate the effect [115,116].

As already noted in the introduction, we may treat only the third generation as effectively supersymmetrized, a premise that is also supported by general bottom-up approaches [114,117]. The low-energy spectrum can be further simplified by assuming that the left-handed superpartners are at least an order of magnitude heavier. The trilinear terms associated with the λ and λ' couplings that are relevant to our discussion and expanded in standard four-component Dirac notation are then

$$\mathcal{L}_\lambda = -\frac{1}{2}\lambda_{ij3}(\tilde{\tau}^*_R \bar{\nu}^c_{Ri} \ell_{Lj} - (i \leftrightarrow j)) + \mathrm{H.c.}, \quad (3)$$

$$\mathcal{L}_{\lambda'} = -\lambda'_{ij3}(\tilde{b}^*_R \bar{\nu}^c_{Ri} d_{Lj} - \tilde{b}^*_R \bar{\ell}^c_{Ri} u_{Lj}) + \mathrm{H.c.} \quad (4)$$

Here, it is also worth mentioning that since direct searches at LHC have been unfruitful so far [118], a "vanilla" MSSM scenario with at least 10% fine-tuning is ruled out [119]. The exploration of nonminimal realizations of SUSY with reduced missing energy signatures, such as RPV SUSY, as viable model building directions is therefore prominent [120–122]. As a matter of fact, our scenario is similar to the effective RPV SUSY model studied in Ref. [122], where the first two generations of squarks decouple from the low-energy spectrum. This is the most successful model in evading LHC bounds for a natural parameter space with a

[1]Historically, the $U(2)$ flavor symmetries have strong ties with SUSY as their initial proposal intended to solve the "flavor problem" of the MSSM [65,66]. This is also true for the WIMP paradigm, since the LSP in R-parity conserving SUSY has been cherished as the prototype of a WIMP particle and a point of reference for direct searches.

[2]See footnote 1.

messenger scale of SUSY breaking 20 TeV $\lesssim \Lambda <$ 100 TeV considered by the authors.

B. Supersymmetric flavored dark matter

We extend the matter content of the MSSM introducing a vectorlike DM flavor multiplet X, $\bar{X}$, and a vectorlike mediator Y, $\bar{Y}$. The requirement that X is a gauge singlet and couples to the left-handed leptons fixes the quantum numbers of the new superfields. It follows, that the mediator is charged under the MSSM gauge group. The most general superpotential relevant to the new superfields can be expressed as

$$W_{\rm DM} = \hat{M}_X X\bar{X} + \hat{M}_Y Y\bar{Y} + \hat{\lambda}_{ij} X_i Y L_j, \tag{5}$$

where i, $j = 1, 2, 3$ denote again flavor indices.

The crucial difference with nonsupersymmetric versions of flavored DM is that the $\hat{\lambda}$ term is the only interaction that we are permitted to include at renormalizable level. For instance, the so-called Higgs portal of scalar DM models, i.e., a scalar cubic interaction between X and the Higgs, is absent. This is an important point, given the fact that such an interaction is strongly constrained by direct detection searches [123] and in nonsupersymmetric scalar DM models one must set the coupling arbitrarily to zero.

As far as the mass terms are concerned, they are obviously nonholomorphic and indeed their origin lies in terms of the Kähler potential that can be associated with the soft SUSY breaking scale in a way analogous to the Giudice-Masiero mechanism [124]. In synergy with noncanonical kinetic terms, which are expanded as functions of flavor spurions, a large mass splitting between X_3 and the nearly degenerate X_1 and X_2 can be obtained [71]. In addition, soft-breaking terms in the hidden sector produce an additional mass splitting between the scalar and fermionic components. As a result, the scalar component χ of X_3 can be the lightest DM state and together with the fermion component ψ of Y, they build the term

$$\mathcal{L}_{\hat{\lambda}} = \hat{\lambda}_{3j}\bar{\ell}_{Lj}\chi\psi + \text{H.c.}, \tag{6}$$

which is the interaction term relevant to low-energy phenomenology.

Regarding the DM stabilization, we notice that because X is leptophilic and the flavor-breaking sources are not MFV type, we cannot apply the mechanism of the residual Z_3 symmetry that exists for quark-flavored DM [69,76]. One can envision alternatives in an extended hidden sector with its own gauge symmetries, but this discussion is beyond the scope of the current paper. We shall simply assume a Z_2 symmetry, under which X and Y are odd and their direct decay to SM particles is forbidden, as it is customary in simplified models of leptophilic dark matter [80,82,83,86–90].

C. Flavor structure

Following EFT approaches [18,22,31,32], a non-Abelian flavor symmetry $U(2)_q \times U(2)_\ell$ was employed in Ref. [58]. Under the assumption that it is spontaneously broken by the vacuum expectation values of two different sets of flavon fields, one quark- and one lepton-flavored, the observed fermion mass hierarchy and the phenomenologically viable hierarchy of RPV couplings are reproduced [125]. Nevertheless, such a breaking pattern is against the idea of gauge coupling unification.[3] It is thus suitable to adopt a different version of the $U(2)^2$ flavor symmetry group that commutes with $SU(5)$, which is contained in all GUT groups. In terms of the $\mathbf{10}_i(T_i) \oplus \bar{\mathbf{5}}_i(\bar{F}_i)$ $(i = 1, 2, 3)$ representations of $SU(5)$, the plausible choice is the flavor symmetry $U(2)_T \times U(2)_{\bar{F}}$ [126], under which the matter superfields transform as

$$\begin{aligned} &(T_1, T_2) \sim (\mathbf{2}, \mathbf{1}), \qquad && T_3 \sim (\mathbf{1}, \mathbf{1}), \\ &(\bar{F}_1, \bar{F}_2) \sim (\mathbf{1}, \mathbf{2}), \qquad && \bar{F}_3 \sim (\mathbf{1}, \mathbf{1}). \end{aligned} \tag{7}$$

In a minimal fashion, we assign $U(2)_{\bar{F}}$ charge to the doublet consisting of the first two generations of X.

The $SU(5)$-invariant Yukawa Lagrangian

$$\begin{aligned} \mathcal{L}_Y = {} & y_t T_3 T_3 H_5 + y_t x_t \mathbf{T}\mathbf{V}_T T_3 H_5 + \mathbf{T}\Delta_T \mathbf{T} H_5 + y_b T_3 \bar{F}_3 H_{\bar{5}} \\ & + y_b x_b \mathbf{T}\mathbf{V}_T \bar{F}_3 H_{\bar{5}} + \mathbf{T}\Delta_{T\times\bar{F}}\bar{\mathbf{F}} H_{\bar{5}} \end{aligned} \tag{8}$$

is also kept flavor-invariant by ascribing to the spurions $\mathbf{V}_T$, Δ_T, and $\Delta_{T\times\bar{F}}$ the appropriate transformation properties. The masses and the mixings in the low-energy limit are then qualitatively understood[4] with the following alignment of the spurions in flavor space:

$$\begin{aligned} &\mathbf{V}_T = (\,0 \quad \epsilon\,)^T, \qquad \Delta_T = \begin{pmatrix} 0 & \epsilon' \\ -\epsilon' & \epsilon\rho \end{pmatrix}, \\ &\Delta_{T\times\bar{F}} = \begin{pmatrix} 0 & \epsilon' \\ -\epsilon' & \epsilon \end{pmatrix}, \end{aligned} \tag{9}$$

the symmetry breaking parameters $\epsilon \approx 0.025$ and $\epsilon' \approx 0.004$ and the higher order correcting parameter $\rho \approx 0.02$ [128].

[3]Note that the beyond-the-MSSM elements postulated in this work do not spoil gauge coupling unification. In particular, RPV interactions even in the limit where the first two generations are decoupled, do not alter the RG evolution up to a shift of the unified coupling value [56] and if the SM-charged mediator Y is embedded in a complete GUT multiplet, e.g., for $SU(5)$ in an antifundamental $\bar{\mathbf{5}}$, then unification is still preserved.

[4]The correct Yukawa matrices are derived only after further refinement of Eq. (8) by including a term of the form $\mathbf{T}\Delta'_{T\times\bar{F}}\bar{\mathbf{F}}H_{\bar{45}}$ that generates different $\mu - s$ and $e - d$ masses and leads to the Georgi-Jarlskog mass relation [127].

All trilinear terms in the superpotential (2) and (5) can be converted to holomorphic flavor singlets by appropriately contracting the matter superfields with the above spurions and an additional spurion $\mathbf{V}_{\bar{F}}$ transforming as $(\mathbf{1},\bar{\mathbf{2}})$. In retrospect, we know that the $b \to s\ell^+\ell^-$ anomalies imply a sizeable coupling λ_{323}, possibly of order $\mathcal{O}(1)$. Since there is no term of the form $\bar{\mathbf{F}}\mathbf{V}_{\bar{F}}\bar{F}_3$ in Eq. (8), we have the freedom to write $\mathbf{V}_{\bar{F}} = (0\epsilon_{\bar{F}})^T$ with $\epsilon_{\bar{F}} \approx 1$. As a result of this symmetry and symmetry-breaking ansatz, we achieve a flavor structure similar to the one proposed in [58], but this time with a more appealing theoretical justification. Last, but not least, a thorough study of the connection between the RPV trilinear and the Yukawa couplings in the context of $SU(5)$ may reveal the conditions under which the relation $\lambda_{323} \approx \lambda'_{233} \approx \lambda'_{333}$ is a prediction of the model [129].

III. OBSERVABLES

In this section, we analyze the impact of the RPV and DM interactions on low-energy observables. It turns out that the relevant processes are those that receive NP contributions dependent on the unsuppressed couplings λ_{323}, λ'_{233}, λ'_{333}, $\hat{\lambda}_{32}$, and $\hat{\lambda}_{33}$ or at least by the ϵ-suppressed couplings λ'_{223} and λ'_{323}. The respective experimental values and upper bounds are listed in Table I.

A. B mesons

The processes that involve the B meson are affected solely by RPV interactions. To begin with, one can build four-fermion, semileptonic operators that generate contributions to the decay of a bottom quark to second-generation quarks from the trilinear terms in (4) by a tree-level sbottom exchange (see Fig. 1). Working in the mass eigenbasis for the down-type quarks, the effective Lagrangians read

TABLE I. Experimental values and SM predictions for the observables used in the numerical analysis.

Observable	Experimental value
$r_{D^{(*)}}$	1.139 ± 0.053[5]
$\delta C_9^\mu = -\delta C_{10}^\mu$	-0.46 ± 0.10 [63]
$R_{B\to K^{(*)}\nu\bar{\nu}}$	<2.7 [130]
C_{B_s}	1.070 ± 0.088 [131]
ϕ_{B_s}	$(0.054 \pm 0.951)°$ [131]
ΔM_{B_d}	$(3.327 \pm 0.013) \times 10^{-13}$ GeV [132]
$\frac{a_\tau}{a_e}$	1.0019 ± 0.0015 [133]
$R_\tau^{\tau/\mu}$	1.0022 ± 0.0030 [134]
$\mathcal{B}(\tau \to \mu\mu\bar{\mu})$	$<2.1 \times 10^{-8}$ [133]
$\mathcal{B}(\tau \to \mu\gamma)$	$<4.4 \times 10^{-8}$ [133]

[5]The value for $r_{D^{(*)}}$ is calculated according to Eq. (14) as the fraction of the weighted average of the R_D and R_{D^*} most recent experimental world average [5] over the weighted average of the $R_D^{\rm SM}$ and $R_{D^*}^{\rm SM}$ predictions [6,7].

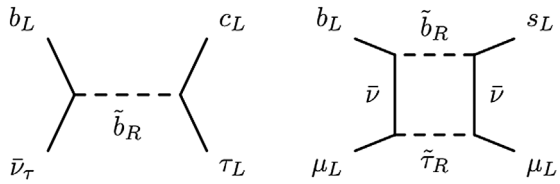

FIG. 1. The principle tree-level and box diagrams that generate contributions to the charged- and neutral-current B-physics anomalies, respectively.

$$\mathcal{L}(b \to c\ell\bar{\nu}_\ell) = -\frac{4G_F}{\sqrt{2}} V_{cb}(\delta_{ii'} + \Delta^c_{ii'})\bar{\ell}^{i'}_L \gamma^\mu \nu^i_L \bar{c}_L \gamma_\mu b_L, \tag{10}$$

$$\mathcal{L}(b \to s\nu\bar{\nu}) = -\frac{4G_F}{\sqrt{2}} \frac{\alpha_{\rm em}}{2\pi s_W^2} X_t V^*_{ts} V_{tb}(\delta_{ii'} + X^s_{ii'})\bar{\nu}^{i'}_L \gamma^\mu \nu^i_L \bar{s}_L \gamma_\mu b_L, \tag{11}$$

where

$$\Delta^c_{ii'} = \sum_{j'=s,b} \frac{\sqrt{2}}{4G_F} \frac{\lambda'_{i33}\lambda'^*_{i'j'3}}{2m^2_{\tilde{b}_R}} \frac{V_{cj'}}{V_{cb}}, \tag{12}$$

$$X^s_{ii'} = -\frac{\pi s_W^2}{\sqrt{2}G_F \alpha_{\rm em} X_t V^*_{ts} V_{tb}} \left(\frac{\lambda'_{i33}\lambda'^*_{i'23}}{2m^2_{\tilde{b}_R}}\right), \tag{13}$$

and $X_t = 1.469 \pm 0.017$ is a SM loop function [135]. The processes of interest are the charged-current $b \to c\tau\nu$ anomaly and the $B \to K^{(*)}\nu\bar{\nu}$ decay. The NP effects are probed by the ratios [54]

$$r_{D^{(*)}} = \frac{R_{D^{(*)}}}{R^{\rm SM}_{D^{(*)}}} = \frac{|1 + \Delta^c_{33}|^2 + |\Delta^c_{23}|^2}{\frac{1}{2}(1 + |1 + \Delta^c_{22}|^2 + |\Delta^c_{32}|^2)} \quad \text{and} \tag{14}$$

$$R_{B\to K^{(*)}\nu\bar{\nu}} = \frac{\mathcal{B}(B \to K^{(*)}\nu\bar{\nu})}{\mathcal{B}(B \to K^{(*)}\nu\bar{\nu})_{\rm SM}} = \sum_{i=\mu,\tau} \frac{1}{3}|1 + X^s_{ii}|^2 + \sum_{i\neq i'} \frac{1}{3}|X^s_{ii'}|^2. \tag{15}$$

The reported enhancement of $r_{D^{(*)}}$ favors large (resp. small) values for the coupling $|\lambda'_{333}|$ (resp. $|\lambda'_{233}|$) and the coupling combination $\lambda'_{333}\lambda'^*_{323}$ (resp. $\lambda_{233}\lambda'^*_{223}$), while $R_{B\to K^{(*)}\nu\bar{\nu}}$ sets a strong upper bound on the sum of the same coupling combinations.

The effective Lagrangian describing the neutral-current $b \to s\ell\bar{\ell}$ decay is parametrized as

$$\mathcal{L}(b\to s\ell\bar{\ell}) = \frac{4G_F}{\sqrt{2}}\frac{\alpha_{\rm em}}{4\pi}V_{tb}V_{tb}^*[(C_9^\ell+\delta C_9^\ell)\bar{\ell}\gamma^\mu\ell\bar{s}_L\gamma_\mu b_L + (C_{10}^\ell+\delta C_{10}^\ell)\bar{\ell}\gamma^\mu\gamma_5\ell\bar{s}_L\gamma_\mu b_L + (C_9^{\prime\ell}+\delta C_9^{\prime\ell})\bar{\ell}\gamma^\mu\ell\bar{s}_R\gamma_\mu b_R + (C_{10}^{\prime\ell}+\delta C_{10}^{\prime\ell})\bar{\ell}\gamma^\mu\gamma_5\ell\bar{s}_R\gamma_\mu b_R]. \quad (16)$$

In our framework, the operator $\bar{\mu}_L^{i'}\gamma^\mu\mu_L^i\bar{d}_R^k\gamma_\mu d_R^{k'}$ is generated at tree-level and the operator $\bar{\mu}_L^{i'}\gamma^\mu\mu_L^i\bar{d}_L^k\gamma_\mu d_L^{k'}$ at one-loop level [55], giving rise to the correlations $\delta C_9^\mu = -\delta C_{10}^\mu$ and $\delta C_9^{\prime\mu} = -\delta C_{10}^{\prime\mu}$.

Let us examine first the tree-level case,

$$\delta C_9^{\prime\mu} = -\delta C_{10}^{\prime\mu} = \frac{\pi\sqrt{2}}{G_F\alpha_e}\frac{1}{V_{tb}V_{ts}^*}\frac{\lambda'_{232}\lambda'_{233}}{4m^2_{\tilde{t}_L}}. \quad (17)$$

The flavor symmetry expectation is $\lambda'_{232}\lambda'_{233}\sim\epsilon_{\bar{F}}^2\epsilon\approx 0.025$ and hence $\delta C_9'\approx(8\times10^6\ \text{GeV}^2)/\text{m}^2_{\tilde{t}_L}$. The operator is disfavored as an explanation for the anomalies [63], which implies that the left-handed stop has to be heavier than a few TeV, as already assumed in Sec. II A. Concretely, the global fit result $\delta C_9^{\prime\mu} = -\delta C_{10}^{\prime\mu}\lesssim 0.12$ is satisfied for $m^2_{\tilde{t}_L}\gtrsim 8$ TeV. We also note, that for this reason the solutions of Refs. [55,57] for the $R_K^{(*)}$ anomaly cannot be applied.

Next, the NP effect at one-loop level is

$$\delta C_9^\mu = -\delta C_{10}^\mu = -\frac{m_t^2}{16\pi\alpha_{\rm em}}\frac{|\lambda'_{233}|^2}{m^2_{\tilde{b}_R}} - \frac{\lambda'_{i33}\lambda'^*_{i23}|\lambda'_{2j3}|^2}{64\sqrt{2}G_F\pi V_{tb}V_{ts}^*\alpha_{\rm em}m^2_{\tilde{b}_R}} - \frac{\lambda'_{333}\lambda'^*_{323}|\lambda_{323}|^2}{64\sqrt{2}G_F\pi V_{tb}V_{ts}^*\alpha_{\rm em}m^2_{\tilde{b}_R}}\frac{\log(m^2_{\tilde{b}_R}/m^2_{\tilde{\tau}_R})}{m^2_{\tilde{b}_R}-m^2_{\tilde{\tau}_R}}. \quad (18)$$

The first term corresponds to a box diagram with a W boson, a sbottom and two tops in the loop, the second to a box with two sbottoms and two tops, and the third to a box with a sbottom, a stau, and two tau neutrinos (see Fig. 1). The first two terms become negligible due to the above-mentioned constraints from the tree-level processes. The third term provides the principal contribution to the anomaly and it is mainly constrained by purely leptonic processes (see next Sec. III B).

Box diagrams with two sbottoms and two tau neutrinos can also affect the $B_s-\bar{B}_s$ mixing [57] (see the Appendix A 1) and impose similar constraints to the ones from $R_{B\to K^{(*)}\nu\bar{\nu}}$ yet slightly weaker.

As a final remark, we point out that the recent analysis in [62] considers also the likelihood in the space of pairs of WCs. It is suggested that the $\delta C_9^\mu = -\delta C_{10}^\mu$ solution is complemented by a nonvanishing, lepton universal, negative contribution δC_9^U. The statistical significance of this scenario is as of now not overwhelming and we do not take it into account here. If the tendency persists, we have verified that the RPV framework can also accommodate it by the inclusion of loop-diagrams with light left-handed tau sneutrinos around the TeV scale. As a bonus, it is possible to explain partially the anomalous magnetic dipole moment of the muon (see Appendix A 3). However, the price to be paid is the abandonment of our flavor symmetry. In particular, the operator $(\bar{b}_R^\alpha s_L^\alpha)(\bar{b}_L^\beta s_R^\beta)$ is generated by a sneutrino $\tilde{\nu}_L$ tree-level exchange and the corresponding WC, $C_{B_s}^{LR} = \frac{\lambda'_{332}\lambda'^*_{323}}{2m^2_{\tilde{\nu}_L}}$ is restricted to be less than 10^{-4} TeV^{-2} by the $B_s-\bar{B}_s$ mixing bounds [136]. We expect $\lambda'_{323}\sim\epsilon\approx 0.025$ and hence for $m_{\tilde{\nu}_L}=1$ TeV, we get $\lambda'_{332}\lesssim 6\times10^{-3}$, which is in contradiction to the flavor symmetry expectation $\lambda'_{332}\sim\epsilon_{\bar{F}}\approx 1$.

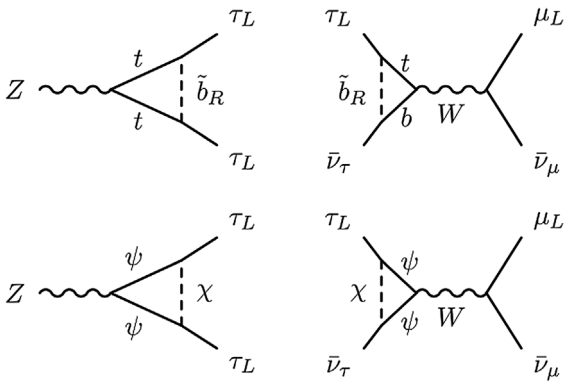

FIG. 2. The triangle and W-penguin diagrams involving RPV and DM interactions that generate contributions to the $\frac{a_\tau}{a_e}$ and $R_\tau^{\tau/\ell}$ observables, respectively. There are two more diagrams involving RPV interactions which result by exchanging the SM quarks with the sbottom (since it also couples to the gauge bosons) in the loop.

B. $Z\to\ell\bar{\ell}'$ coupling and LFV τ decays

The main obstacles to a combined solution to the anomalies in the generic RPV scenario are the stringent constraints from the Z boson decay to a dilepton pair and the charged-current leptonic tau decay to a lepton and neutrinos [137,138]. On the one hand, the triangle diagrams involving the sbottom and the top generate a positive contribution to the leptonic Z coupling that saturates the experimental bound already for order $\mathcal{O}(1)$ values of λ'_{333}. On the other hand, the tree-level stau exchange implies an unacceptably large shift of the $\tau\to l\nu\bar{\nu}$ decay rate [139], unless the stau mass is of order 10 TeV. The third term in (18) becomes also negligible and thus the $R_{K^{(*)}}$ anomaly remains unresolved. Moreover, no cancellation between the positive tree-level amplitude and the negative W penguin diagrams involving the sbottom and the top can be invoked due to the previous bounds on λ'_{333} from the Z coupling.

We stress that the necessity of a cancellation between the tree-level purely leptonic interaction and the leptoquark

RGE effects appearing at one-loop level is already anticipated by the EFT analysis based on $U(2)$ flavor symmetries [32]. Motivated by this analysis, we examine how the DM interactions may alter the above conclusions. Let us write down the relevant observables, i.e., the ratio of Z boson axial-vector coupling,

$$\frac{a_\tau}{a_e} = 1 - \frac{3m_t^2}{16\pi^2}\frac{|\lambda'_{333}|^2}{m^2_{\tilde{b}_R}}\left(\log\left(\frac{m^2_{\tilde{b}_R}}{m_t^2}\right) - 1\right) + (1-4s_W^2)\frac{|\hat{\lambda}_{33}|^2}{16\pi^2}\left(\frac{m_\chi^2}{m_\psi^2}\log\left(\frac{m_\chi^2}{m_\psi^2}\right) + 1\right), \quad (19)$$

and the following ratio of leptonic decay branching ratios at leading order:

$$R_\tau^{\tau/\ell} = \frac{\mathcal{B}(\tau \to \ell\nu\bar{\nu})_{\rm exp}/\mathcal{B}(\tau \to \ell\nu\bar{\nu})_{\rm SM}}{\mathcal{B}(\mu \to e\nu\bar{\nu})_{\rm exp}/\mathcal{B}(\mu \to e\nu\bar{\nu})_{\rm SM}} \simeq 1 + \frac{\sqrt{2}}{4G_F}\frac{|\lambda_{323}|^2}{m^2_{\tilde{\tau}_R}} - \frac{3m_t^2}{16\pi^2}\frac{|\lambda'_{333}|^2}{m^2_{\tilde{b}_R}}\left(\log\left(\frac{m^2_{\tilde{b}_R}}{m_t^2}\right) - \frac{1}{2}\right) - \frac{\hat{\lambda}_{32}\hat{\lambda}^*_{33}}{8\pi^2}\left(\frac{m_\chi^2}{m_\psi^2}\log\left(\frac{m_\chi^2}{m_\psi^2}\right) + 1\right). \quad (20)$$

We observe that the inclusion of the new scalar particle χ together with the mediator ψ can potentially improve the situation. Not only, do they enter a triangle diagram that contributes to $\frac{a_\tau}{a_e}$ with an opposite sign to the RPV term, but also a W penguin diagram that can facilitate further the cancellation in $R_\tau^{\tau/\ell}$. It should be noted that, if the DM particle were the Dirac fermion in X_3 the contribution to the Z coupling would be negligible (see Fig. 2).

In the presence of the DM interactions, the effects on two more LFV τ decays should be taken into account. In particular, Z penguin diagrams with either the sbottom and the top [57] or the χ and the ψ in the loop may pose a problem with regard to the SM forbidden $\tau \to \mu\mu\bar{\mu}$ decay[6] and triangle diagrams with the same particles [140,141] regarding the radiative $\tau \to \mu\gamma$ decay (see Appendix A 3).

C. Relic abundance and dark matter direct detection

The DM particle couples directly to leptons and therefore the main self-annihilation channels are $\bar{\chi}\chi \to \bar{\ell}\ell$ and $\bar{\chi}\chi \to \bar{\nu}_\ell\nu_\ell$ with $\ell = \mu, \tau$. Because χ is a scalar particle, the effective cross section is p-wave suppressed [83],

$$\frac{1}{2}\langle\sigma v\rangle = \frac{1}{2}\left[\frac{(|\hat{\lambda}_{32}|^2 + |\hat{\lambda}_{33}|^2)m_\chi^2}{48\pi(m_\psi^2 + m_\chi^2)^2}v^2\right] \equiv pv^2, \quad (21)$$

[6]There are also box diagrams [57] and photon penguin [140] diagrams that contribute to this decay, but we have explicitly checked that they are subleading.

where $v \sim 3$ is the DM velocity at freeze-out. The relic abundance can be estimated following the calculation in Ref. [70]. Coannihilation effects are irrelevant since the rest of the DM generations are taken to be heavier.

Concerning direct detection, the dominant contribution for DM scattering off nucleons is generated via a penguin diagram involving leptons and the charged mediator in the loop and a virtual photon exchange. The respective dimension-six operator is called charge-radius operator,

$$\mathcal{L}_{\text{charge-radius}} = ib_\chi\partial_\mu\chi^*\partial_\nu\chi F^{\mu\nu}, \quad (22)$$

where

$$b_\chi = \sum_{\ell=\mu,\tau}\frac{|\hat{\lambda}_{3\ell}|^2 e}{16\pi^2 m_\psi^2}\left(1 - \frac{2}{3}\log\left(\frac{m_\ell^2}{m_\psi^2}\right)\right). \quad (23)$$

The spin-independent DM-nucleus differential scattering cross section is then [83]

$$\frac{d\sigma}{dE_R} = \frac{Z^2e^2b_\chi^2 m_T}{16\pi v^2}F_E^2(q^2). \quad (24)$$

Here, $E_R = |\vec{q}|^2/2m_T$ is the recoil energy; v is the DM velocity in the lab frame; m_T is the mass, Z the atomic number and $F_E(q^2)$ the electric form factor of the target nucleus [142]. Equation (24) has the same E_R- and v^2-dependence as the ordinary spin-independent cross section for a contact interaction, we can directly map the latest, most stringent exclusion limits, as published by the XENON1T Collaboration [143], onto limits on the parameter space of the current model. Since the virtual photon couples only to protons inside the nucleus, a rescaling with Z^2/A^2 is necessary in order to account for the resulting isospin violation. We also derive projections for XENONnT, which is the next upgrade step of XENON1T and will increase the target mass to 5.9t, by assuming the same efficiency profile.

Last, we mention that indirect detection signals of scalar DM are too small to be observed due to the p-wave suppression of the cross section [144].

D. Collider searches

We highlight the basic aspects of the high-p_T searches for the new particles. The direct comparison with analyses that study the analogous EFT operators offers the possibility to set present and future bounds for their masses and interactions.

(i) $\tilde{\boldsymbol{b}}_{\boldsymbol{R}}$: Crossing symmetry dictates that an explanation for $R_{D^{(*)}}$ is unambiguously connected to the scattering $bc \to \tau\bar{\nu}$. The data from the mono-tau signature $pp \to \tau_h X + \text{MET}$ at LHC set upper bounds on the WC of the effective operator generated by a scalar leptoquark $S_1 \sim (\bar{\mathbf{3}}, \mathbf{1})_{1/3}$ exchange [56,145], which

for our case translates into $\Delta^c_{33} < 0.32$ [see Eq. (12)]. The prognosis for the HL-LHC (3000 fb^{-1}) gives $\Delta^c_{33} < 0.1$.

(ii) $\tilde{\tau}_R$: Depending on the nature of the LSP, the possible signatures involving the stau are classified in Ref. [146]. The best limits in RPV searches using simplified models yield $m_{\tilde{\tau}_R} > 300$ GeV.

(iii) χ & ψ: The mediator ψ can be pair-produced at LHC via Drell-Yan processes, i.e., a Z boson or photon exchange, with dilepton plus missing energy signature $l_i^+ l_j^- + \text{MET}$. The cross sections are larger than that of fermion DM models, because there are more helicity states for the fermionic mediator. If the leptons have the same flavor, one can recast slepton searches and extrapolate the limits $m_\chi > 300$ GeV and $m_\psi > 500$ GeV [84]. Likewise, $\psi\bar{\psi}$ direct production is possible at LEP, but the bounds are even weaker [144]. Other channels accessible at future muon colliders that are relevant to our setup could be $\mu^+\mu^- \to \chi\bar{\chi}\gamma$ at tree-level with mono-photon search signature and $\mu^+\mu^- \to l_i^+ l_j^- \gamma$ at one-loop level with multiflavor lepton final state (in analogy to the discussion in Ref. [89] for LEP).

IV. PHENOMENOLOGICAL ANALYSIS

The preferred region of the parameter space is determined by performing a minimization of the χ^2 distribution composed by the observables of Sec. III. We use the experimental data of Table I, the XENON1T exclusion limits [143], the mass lower bounds set by collider searches (see Sec. III D), and the necessary SM input [133]. The values of the couplings are taken to be less than $\sqrt{4\pi}$, while the complex phases are not directly constrained. As a matter of fact, what enters the expressions of the various observables are the absolute values of single couplings or coupling combinations. The only parameter that may potentially probe directly the size of CP-violating phases is ϕ_{B_s} yet the overall flavor suppression excludes this possibility at the moment.[7]

The best-fit point is presented in Table II. The improvement of the total χ^2 with respect to the SM limit $\chi^2(x_{\rm SM}) - \chi^2(x_{\rm BF}) \simeq 33 - 5 = 27$ reflects the resolution of the anomalies. This is also evident in the Fig. 3, where the 68% CL and 95% CL regions of the $r_{D^{(*)}}$ and δC_9^μ observables in the $(\lambda'_{333}, \lambda'_{323})$, $(\lambda'_{333}, m_{\tilde{b}_R})$, and $(\lambda'_{333}, m_{\tilde{\tau}_R})$ planes are shown together with the 2σ exclusion contours from the other low-energy observables. We observe that a large fraction of the parameter space becomes available due the cancellation mechanism in Sec. III B. In particular, the coupling λ'_{333} reaches now higher values compared with the generic RPV scenario [56] and the bounds on $B_s - \bar{B}_s$ mixing and $R_{B\to K^{(*)}\nu\bar{\nu}}$ are still satisfied thanks to the flavor suppression in λ'_{323}. Moreover, the stau can be relatively light enhancing adequately the last term in Eq. (18). Both $R_{D^{(*)}}$ and $R_{K^{(*)}}$ are then in good agreement with the present central values and the mass spectrum is more natural with all the right-handed superparters, χ and ψ within the same mass range of a few TeV. However, due to the sensitivity of $R_\tau^{\tau/\ell}$ to the cancellation, $R_{K^{(*)}}$ can only be accommodated in a concrete band of the $(\lambda'_{333}, m_{\tilde{\tau}_R})$ plane, which for this solution is located around a stau mass of approximately 2 TeV. By varying the coupling λ_{323} and the DM parameters, the position of the band can be moved to the left as low as ∼1.4 TeV before abandoning the 1σ region for δC_9^μ (see the values in brackets in Table II). As for the couplings λ'_{223} and λ'_{233}, the first is flavor suppressed and does not affect the fit and the latter is primarily constrained by the bounds on LFV τ decays (see Eqs. (A7)–(A12)).

Regarding the DM interactions, we notice that the coupling $\hat{\lambda}_{32}$ appears only in a product combination with the coupling $\hat{\lambda}_{33}$ in the observables of Sec. III B and the single-coupling bounds from, e.g., $\frac{a_\mu}{a_e}$, are satisfied for any order $\mathcal{O}(1)$ value. Consequently, it is convenient to use the benchmark $\hat{\lambda}_{32} = 1$ and include only $\hat{\lambda}_{33}$ in the fit. The region in the (m_ψ, m_χ) plane that can give rise to the correct relic abundance is shown in Fig. 4. The present direct detection and LFV bounds allow for a DM mass 700 GeV $< m_\chi <$ 1.5 TeV, and we have explicitly verified that the cancellation mechanism is applicable for the whole mass range by readjusting the rest of the parameters.

TABLE II. The best-fit point for the couplings along with the flavor suppression factors and the particle masses. The entries marked with a dagger are not determined by the fit, but are rather benchmark points (see text). The values in the brackets denote a fit-point that allow for a smaller stau mass still within the 1σ region for the anomalies.

RPV and DM couplings	Best-fit point	Flavor suppression	Total value
λ_{323}	3 [1.9]	$\epsilon_{\bar{F}}$	3 [1.9]
λ'_{223}	$1^\dagger$ [1]	$\epsilon_{\bar{F}}\epsilon$	0.03 [0.03]
λ'_{233}	0.7 [1]	$\epsilon_{\bar{F}}$	0.7 [1]
λ'_{323}	2.4 [3.3]	ϵ	0.07 [0.1]
λ'_{333}	2.3 [2.1]	1	2.3 [2.1]
$\hat{\lambda}_{32}$	$1^\dagger$ [2]	$\epsilon_{\bar{F}}$	1 [2]
$\hat{\lambda}_{33}$	3.5 [2.5]	1	3.5 [2.5]

Masses	Best-fit point [GeV]
$m_{\tilde{b}_R}$	1600 [1800]
$m_{\tilde{\tau}_R}$	2700 [1400]
m_χ	700 [1000]
m_ψ	2000 [1900]

[7]We estimate the impact of complex phases according to Eq. (A4) and get $\phi_{B_s} \in [-0.4°, 0.4°]$, which is well within the current experimental limits.

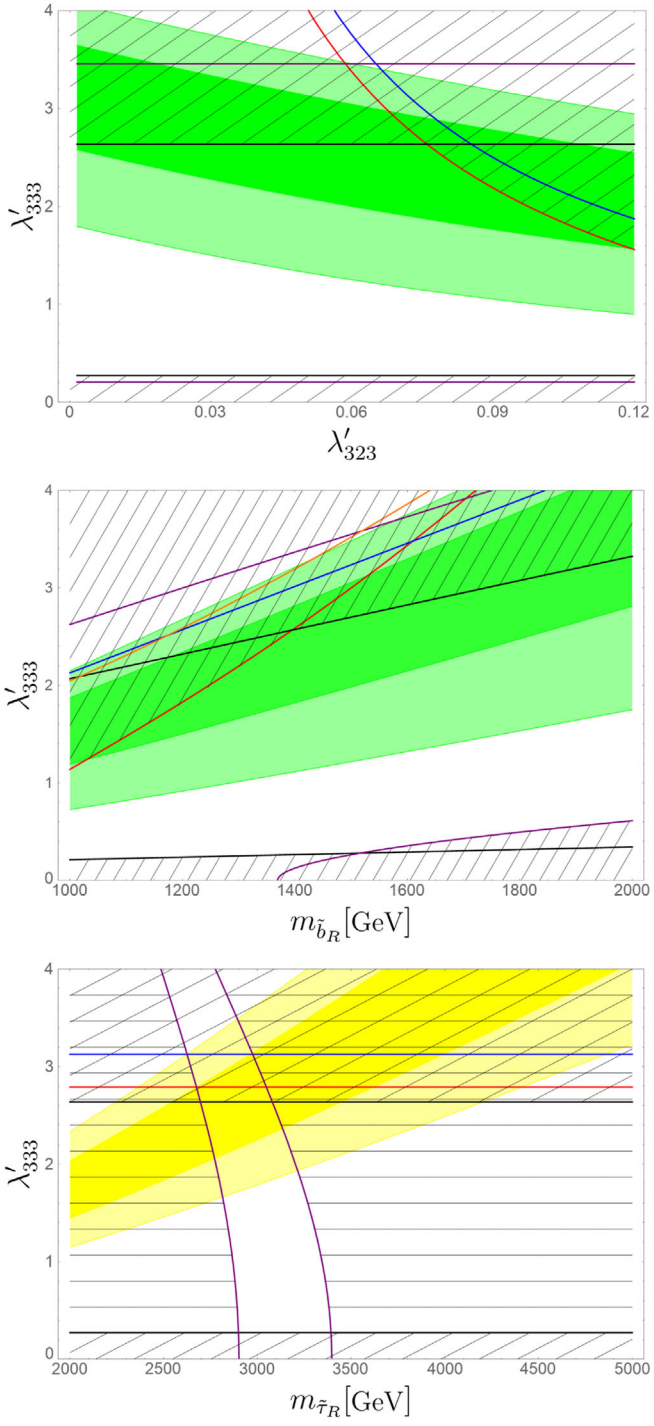

FIG. 3. RPV parameter space compatible with a solution for $r_{D^{(*)}}$ (green) and δC_9^μ (yellow) at 1σ and 2σ around the best-fit point. The hatched region is excluded at 2σ due to the following constraints: $R_{B\to K^{(*)}\nu\bar{\nu}}$ (red), C_{B_s} (blue), $\frac{a_\tau}{a_e}$ (black), $R_\tau^{\tau/\ell}$ (purple), $\mathcal{B}(\tau \to \mu\mu\bar{\mu})$ (orange).

One may additionally quantify the percentage of cancellation needed between the NP terms in $\frac{a_\tau}{a_e}$ and $R_\tau^{\tau/\ell}$ and find that it amounts to approximately 40% and 10%, respectively. This is a rather mild condition and it can

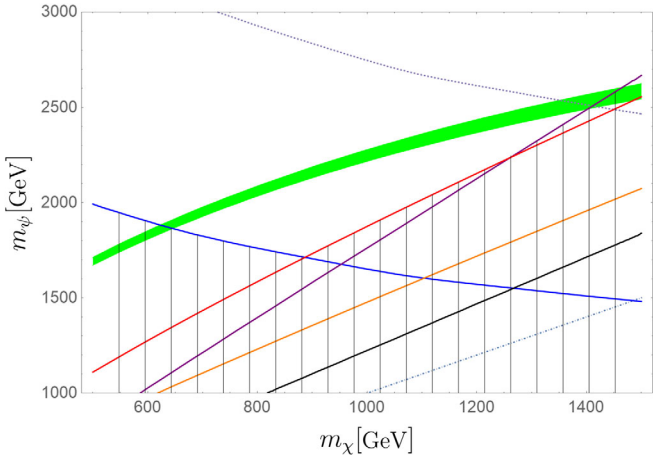

FIG. 4. DM parameter space compatible with the correct relic abundance (green) at 1σ around the best-fit point. The hatched region is excluded at 2σ due to the following constraints: XENON1T exclusion limits (blue), $\frac{a_\tau}{a_e}$ (black), $R_\tau^{\tau/\ell}$ (purple), $\mathcal{B}(\tau \to \mu\gamma)$ (red), $\mathcal{B}(\tau \to \mu\mu\bar{\mu})$ (orange). The dashed line represents the prospective XENONnT exclusion limits.

be fulfilled independently of the relative sign of the couplings. Note that the cancellation in $R_\tau^{\tau/\ell}$ is exactly of the same order as the one predicted by the general EFT analysis [32].

As a final note, we comment on the testability of the model by future experiments. With the most recent world average for the charged-current anomalies [5], we calculate $\Delta_{33}^c \approx 0.065$. The "no-loose theorem" of Ref. [145] no longer applies and there is still an open window for the leptoquark explanation of $R_{D^{(*)}}$, even if there is no discovery after the HL-LHC phase. The situation for the stau and χ is even more inconclusive, since the masses for these particles appear to be out of reach of the LHC. On the other hand, DM direct detection looks much more promising. We see that the bulk of the parameter space for the chosen benchmark will be probed by XENONnT (and other experiments that aim at similar exposure). If the anomalies are univocally confirmed as NP signals, it is worth analyzing the sensitivity of the next generation of colliders to the heavy particles predicted by the model.

V. CONCLUSIONS

In this paper, we further investigate the possibility to provide a simultaneous explanation for the B-physics anomalies within the framework of RPV interactions controlled by an approximate $U(2)^2$ flavor symmetry. As pathfinder we use the observation, established by the general EFT analysis, that a destructive amplitude interference in purely leptonic interactions may cure the tensions with specific LFV observables that put limitations on the viability of the scalar leptoquark solution. Furthermore, we assume that the violation of R-parity necessitates the consideration

of a new hidden sector that contains a DM candidate particle and that this sector is also charged under the same flavor symmetry. We show that in this case, from the plethora of flavored DM models, one particular model that features a leptophilic, scalar DM particle is uniquely singled out and favored from the low-energy fit. It is ensured that all newly introduced particles, interactions, and symmetry breaking patterns are in accordance with the spirit of gauge coupling unification. If the sbottom is the LSP, SUSY may remain elusive for the LHC, whereas experimental validation of the proposed DM interaction by direct detection searches can be expected in the near future.

ACKNOWLEDGMENTS

We thank Gino Isidori, Javier Fuentes-Martin, and Michael Baker for useful discussions and comments on the article. This research was supported in part by the Swiss National Science Foundation under Contract No. 200021-159720.

APPENDIX A: ADDITIONAL FLAVOR CONSTRAINTS

1. $\Delta B = 2$

It is useful to define the effective Hamiltonian,

$$\mathcal{H}(\Delta B=2)^{\mathrm{SM(NP)}} = -C_{B_s}^{\mathrm{SM(NP)}}(\bar{b}_L\gamma^\mu s_L)(\bar{b}_L\gamma_\mu s_L), \tag{A1}$$

where

$$C_{B_s}^{\mathrm{SM}} = -\frac{g^4}{128\pi^2 m_W^2}(V_{tb}V_{ts}^*)^2 S_0(m_t^2/m_W^2),$$
$$C_{B_s}^{\mathrm{NP}} = \frac{\lambda'_{i33}\lambda'^*_{i23}\lambda'_{j33}\lambda'^*_{j23}}{128\pi^2 m_{\tilde{b}_R}^2} \tag{A2}$$

and $S_0(x) = \frac{x(4-11x+x^2)}{4(1-x)^2} - \frac{3x^3\log(x)}{2(1-x)^3}$.

We compare the ratio

$$C_{B_s} = \frac{|\langle B_s^0|\mathcal{H}(\Delta B=2)^{\mathrm{SM+NP}}|\bar{B}_s^0\rangle|}{|\langle B_s^0|\mathcal{H}(\Delta B=2)^{\mathrm{SM}}|\bar{B}_s^0\rangle|} = \left|1+\frac{C_{B_s}^{\mathrm{NP}}}{C_{B_s}^{\mathrm{SM}}}\right| \tag{A3}$$

and the CP-violating phase

$$\phi_{B_s} = \frac{1}{2}\mathrm{Arg}\left(1+\frac{C_{B_s}^{\mathrm{NP}}}{C_{B_s}^{\mathrm{SM}}}\right) \tag{A4}$$

with the measured values.

2. $(g-2)_\mu$

The effective Lagrangian that describes the muon anomalous magnetic dipole moment is

$$\mathcal{L}(\mu\to\mu\gamma) = \frac{e}{4m_\mu}a_\mu\bar{\mu}\sigma_{\alpha\beta}\mu F^{\alpha\beta}, \tag{A5}$$

and the generic expression for leptonic RPV interactions [147] is

$$a_\mu = \frac{m_\mu^2}{96\pi^2}|\lambda_{323}|^2\left(\frac{2}{m_{\tilde{\nu}_L}^2}-\frac{1}{m_{\tilde{\tau}_R}^2}\right). \tag{A6}$$

The discrepancy between the SM prediction and the experiment $\Delta a_\mu = a_\mu^{\mathrm{exp}} - a_\mu^{\mathrm{exp}} = (29.3\pm 9.0)\times 10^{-10}$ requires a positive contribution that is provided by the first term in the above equation.

3. $\tau\to\mu\mu\bar{\mu}$ and $\tau\to\mu\gamma$

The effective Lagrangian and effective amplitude for these processes can be expressed as

$$\mathcal{L}(\tau\to\mu\mu\bar{\mu}) = -g_{LL}^{3\mu}(\bar{\tau}_L\gamma^\mu\mu_L)(\bar{\mu}_L\gamma_\mu\mu_L) - g_{LR}^{3\mu}(\bar{\tau}_L\gamma^\mu\mu_L)(\bar{\mu}_R\gamma_\mu\mu_R), \tag{A7}$$

$$\mathcal{M}(\tau\to\mu\gamma) = -e\frac{m_\tau}{2}\epsilon^\alpha\bar{u}_\mu[i\sigma_{\beta\alpha}q^\beta(a_RP_L+a_LP_R)]u_\tau. \tag{A8}$$

We define

$$g_{LL(LR)}^{3\mu} = \frac{4\pi\alpha_{\mathrm{em}}\kappa_{L(R)}}{c_W^2 s_W^2 m_Z^2}\left[\frac{3m_t^2}{32\pi^2}\frac{\lambda'_{233}\lambda'^*_{333}}{m_{\tilde{b}_R}^2}\left(\log\left(\frac{m_{\tilde{b}_R}^2}{m_t^2}\right)-1\right) - (1-4s_W^2)\frac{|\hat{\lambda}_{33}|^2}{32\pi^2}\left(\frac{m_\chi^2}{m_\psi^2}\log\left(\frac{m_\chi^2}{m_\psi^2}\right)+1\right)\right], \tag{A9}$$

where $\kappa_L = -\frac{1}{2}+s_W^2$, $\kappa_R = s_W^2$, and

$$a_L = -\frac{\hat{\lambda}_{32}\hat{\lambda}_{33}^*}{192\pi^2 m_\psi^2}G(m_\chi^2/m_\psi^2) - \frac{\lambda'_{2i3}\lambda'^*_{3i3}}{64\pi^2 m_{\tilde{b}_R}^2}, \qquad a_R = 0, \tag{A10}$$

where $G(x) = \frac{1}{(1-x)^4}(2-3x-6x^2+x^3+6x\log(x))$. The branching ratios [148]

$$\mathcal{B}(\tau\to\mu\mu\bar{\mu}) = \frac{1}{G_F^2}\left[\frac{|g_{LL}^{3\mu}|^2+|g_{LR}^{3\mu}|^2}{4} + \left(\log\frac{m_\tau^2}{m_\mu^2}-\frac{11}{4}\right)(4\pi\alpha_{\mathrm{em}})^2|a_L|^2 + \Re\left(a_L^* g_{LL}^{3\mu}+\frac{1}{2}a_L^* g_{LR}^{3\mu}\right)(4\pi\alpha_{\mathrm{em}})\right]\mathcal{B}(\tau\to\mu\bar{\nu}_\mu\nu_\tau), \tag{A11}$$

$$\mathcal{B}(\tau\to\mu\gamma) = \frac{48\pi^3\alpha_{\mathrm{em}}}{G_F^2}(|a_L|^2+|a_R|^2)\mathcal{B}(\tau\to\mu\bar{\nu}_\mu\nu_\tau) \tag{A12}$$

must then comply with the respective experimental upper bounds.

[1] J. P. Lees *et al.* (*BABAR* Collaboration), Phys. Rev. D **88**, 072012 (2013).
[2] S. Hirose *et al.* (Belle Collaboration), Phys. Rev. Lett. **118**, 211801 (2017).
[3] R. Aaij *et al.* (LHCb Collaboration), Phys. Rev. Lett. **115**, 111803 (2015); **115**, 159901(A) (2015).
[4] R. Aaij *et al.* (LHCb Collaboration), Phys. Rev. D **97**, 072013 (2018).
[5] G. Caria (Belle Collaboration), in *54th Rencontres de Moriond on Electroweak Interactions and Unified Theories (Moriond EW 2019), La Thuile, Italy* (2019).
[6] F. U. Bernlochner, Z. Ligeti, M. Papucci, and D. J. Robinson, Phys. Rev. D **95**, 115008 (2017); **97**, 059902(E) (2018).
[7] D. Bigi, P. Gambino, and S. Schacht, J. High Energy Phys. 11 (2017) 061.
[8] R. Aaij *et al.* (LHCb Collaboration), J. High Energy Phys. 08 (2017) 055.
[9] R. Aaij *et al.* (LHCb Collaboration), Phys. Rev. Lett. **122**, 191801 (2019).
[10] M. Bordone, G. Isidori, and A. Pattori, Eur. Phys. J. C **76**, 440 (2016).
[11] R. Aaij *et al.* (LHCb Collaboration), J. High Energy Phys. 02 (2016) 104.
[12] S. Wehle *et al.* (Belle Collaboration), Phys. Rev. Lett. **118**, 111801 (2017).
[13] M. Ciuchini, M. Fedele, E. Franco, S. Mishima, A. Paul, L. Silvestrini, and M. Valli, J. High Energy Phys. 06 (2016) 116.
[14] R. Aaij *et al.* (LHCb Collaboration), Phys. Rev. Lett. **120**, 121801 (2018).
[15] R. Watanabe, Phys. Lett. B **776**, 5 (2018).
[16] B. Bhattacharya, A. Datta, D. London, and S. Shivashankara, Phys. Lett. B **742**, 370 (2015).
[17] R. Alonso, B. Grinstein, and J. Martin Camalich, J. High Energy Phys. 10 (2015) 184.
[18] A. Greljo, G. Isidori, and D. Marzocca, J. High Energy Phys. 07 (2015) 142.
[19] L. Calibbi, A. Crivellin, and T. Ota, Phys. Rev. Lett. **115**, 181801 (2015).
[20] M. Bauer and M. Neubert, Phys. Rev. Lett. **116**, 141802 (2016).
[21] S. Fajfer and N. Košnik, Phys. Lett. B **755**, 270 (2016).
[22] R. Barbieri, G. Isidori, A. Pattori, and F. Senia, Eur. Phys. J. C **76**, 67 (2016).
[23] D. Das, C. Hati, G. Kumar, and N. Mahajan, Phys. Rev. D **94**, 055034 (2016).
[24] G. Hiller, D. Loose, and K. Schoenwald, J. High Energy Phys. 12 (2016) 027.
[25] B. Bhattacharya, A. Datta, J.-P. Guévin, D. London, and R. Watanabe, J. High Energy Phys. 01 (2017) 015.
[26] S. M. Boucenna, A. Celis, J. Fuentes-Martin, A. Vicente, and J. Virto, Phys. Lett. B **760**, 214 (2016).
[27] D. Buttazzo, A. Greljo, G. Isidori, and D. Marzocca, J. High Energy Phys. 08 (2016) 035.
[28] S. M. Boucenna, A. Celis, J. Fuentes-Martin, A. Vicente, and J. Virto, J. High Energy Phys. 12 (2016) 059.
[29] R. Barbieri, C. W. Murphy, and F. Senia, Eur. Phys. J. C **77**, 8 (2017).
[30] D. Becirevic, N. Kosnik, O. Sumensari, and R. Z. Funchal, J. High Energy Phys. 11 (2016) 035.
[31] D. Buttazzo, A. Greljo, G. Isidori, and D. Marzocca, J. High Energy Phys. 11 (2017) 044.
[32] M. Bordone, G. Isidori, and S. Trifinopoulos, Phys. Rev. D **96**, 015038 (2017).
[33] A. Crivellin, D. Müller, and T. Ota, J. High Energy Phys. 09 (2017) 040.
[34] Y. Cai, J. Gargalionis, M. A. Schmidt, and R. R. Volkas, J. High Energy Phys. 10 (2017) 047.
[35] E. Megias, M. Quiros, and L. Salas, J. High Energy Phys. 07 (2017) 102.
[36] L. Di Luzio, A. Greljo, and M. Nardecchia, Phys. Rev. D **96**, 115011 (2017).
[37] N. Assad, B. Fornal, and B. Grinstein, Phys. Lett. B **777**, 324 (2018).
[38] L. Calibbi, A. Crivellin, and T. Li, Phys. Rev. D **98**, 115002 (2018).
[39] M. Bordone, C. Cornella, J. Fuentes-Martin, and G. Isidori, Phys. Lett. B **779**, 317 (2018).
[40] R. Barbieri and A. Tesi, Eur. Phys. J. C **78**, 193 (2018).
[41] A. Greljo and B. A. Stefanek, Phys. Lett. B **782**, 131 (2018).
[42] M. Blanke and A. Crivellin, Phys. Rev. Lett. **121**, 011801 (2018).
[43] L. Di Luzio, J. Fuentes-Martin, A. Greljo, M. Nardecchia, and S. Renner, J. High Energy Phys. 11 (2018) 081.
[44] D. Marzocca, J. High Energy Phys. 07 (2018) 121.
[45] J. Kumar, D. London, and R. Watanabe, Phys. Rev. D **99**, 015007 (2019).
[46] D. Guadagnoli, M. Reboud, and O. Sumensari, J. High Energy Phys. 11 (2018) 163.
[47] D. Becirevic, I. Dorsner, S. Fajfer, N. Kosnik, D. A. Faroughy, and O. Sumensari, Phys. Rev. D **98**, 055003 (2018).
[48] M. Bordone, C. Cornella, J. Fuentes-Martin, and G. Isidori, J. High Energy Phys. 10 (2018) 148.
[49] B. Fornal, S. A. Gadam, and B. Grinstein, Phys. Rev. D **99**, 055025 (2019).
[50] S. Bhattacharya, A. Biswas, Z. Calcuttawala, and S. K. Patra, arXiv:1902.02796.
[51] C. Cornella, J. Fuentes-Martin, and G. Isidori, J. High Energy Phys. 07 (2019) 168.
[52] S. Biswas, D. Chowdhury, S. Han, and S. J. Lee, J. High Energy Phys. 02 (2015) 142.
[53] J. Zhu, H.-M. Gan, R.-M. Wang, Y.-Y. Fan, Q. Chang, and Y.-G. Xu, Phys. Rev. D **93**, 094023 (2016).
[54] N. G. Deshpande and X.-G. He, Eur. Phys. J. C **77**, 134 (2017).
[55] D. Das, C. Hati, G. Kumar, and N. Mahajan, Phys. Rev. D **96**, 095033 (2017).
[56] W. Altmannshofer, P. B. Dev, and A. Soni, Phys. Rev. D **96**, 095010 (2017).
[57] K. Earl and T. Gregoire, J. High Energy Phys. 08 (2018) 201.
[58] S. Trifinopoulos, Eur. Phys. J. C **78**, 803 (2018).
[59] Q.-Y. Hu, X.-Q. Li, Y. Muramatsu, and Y.-D. Yang, Phys. Rev. D **99**, 015008 (2019).

[60] R. Barbieri and R. Ziegler, J. High Energy Phys. 07 (2019) 023.
[61] S. Descotes-Genon, L. Hofer, J. Matias, and J. Virto, J. High Energy Phys. 06 (2016) 092.
[62] J. Aebischer, W. Altmannshofer, D. Guadagnoli, M. Reboud, P. Stangl, and D. M. Straub, arXiv:1903.10434.
[63] M. Alguer, B. Capdevila, A. Crivellin, S. Descotes-Genon, P. Masjuan, J. Matias, and J. Virto, Eur. Phys. J. C **79**, 714 (2019).
[64] S. P. Martin, *A Supersymmetry Primer*, Advanced Series on Directions in High Energy Physics Vol. 18 (1998), p. 1.
[65] R. Barbieri, G. R. Dvali, and L. J. Hall, Phys. Lett. B **377**, 76 (1996).
[66] R. Barbieri, G. Isidori, J. Jones-Perez, P. Lodone, and D. M. Straub, Eur. Phys. J. C **71**, 1725 (2011).
[67] J. F. Kamenik and J. Zupan, Phys. Rev. D **84**, 111502 (2011).
[68] J. Kile and A. Soni, Phys. Rev. D **84**, 035016 (2011).
[69] B. Batell, J. Pradler, and M. Spannowsky, J. High Energy Phys. 08 (2011) 038.
[70] Y. Bai and J. Berger, J. High Energy Phys. 11 (2013) 171.
[71] B. Batell, T. Lin, and L.-T. Wang, J. High Energy Phys. 01 (2014) 075.
[72] A. Kumar and S. Tulin, Phys. Rev. D **87**, 095006 (2013).
[73] A. DiFranzo, K. I. Nagao, A. Rajaraman, and T. M. P. Tait, J. High Energy Phys. 11 (2013) 014; 01 (2014) 162(E).
[74] L. Lopez-Honorez and L. Merlo, Phys. Lett. B **722**, 135 (2013).
[75] P. Agrawal, B. Batell, D. Hooper, and T. Lin, Phys. Rev. D **90**, 063512 (2014).
[76] P. Agrawal, M. Blanke, and K. Gemmler, J. High Energy Phys. 10 (2014) 072.
[77] C. Kilic, M. D. Klimek, and J.-H. Yu, Phys. Rev. D **91**, 054036 (2015).
[78] M. Blanke and S. Kast, J. High Energy Phys. 05 (2017) 162.
[79] M. Blanke, S. Das, and S. Kast, J. High Energy Phys. 02 (2018) 105.
[80] P. Agrawal, S. Blanchet, Z. Chacko, and C. Kilic, Phys. Rev. D **86**, 055002 (2012).
[81] P. Agrawal, Z. Chacko, and C. B. Verhaaren, J. High Energy Phys. 08 (2014) 147.
[82] Z.-H. Yu, X.-J. Bi, Q.-S. Yan, and P.-F. Yin, Phys. Rev. D **91**, 035008 (2015).
[83] Y. Bai and J. Berger, J. High Energy Phys. 08 (2014) 153.
[84] S. Chang, R. Edezhath, J. Hutchinson, and M. Luty, Phys. Rev. D **90**, 015011 (2014).
[85] J. Kile, A. Kobach, and A. Soni, Phys. Lett. B **744**, 330 (2015).
[86] A. Hamze, C. Kilic, J. Koeller, C. Trendafilova, and J.-H. Yu, Phys. Rev. D **91**, 035009 (2015).
[87] C.-J. Lee and J. Tandean, J. High Energy Phys. 04 (2015) 174.
[88] P. Agrawal, Z. Chacko, E. C. F. S. Fortes, and C. Kilic, Phys. Rev. D **93**, 103510 (2016).
[89] M.-C. Chen, J. Huang, and V. Takhistov, J. High Energy Phys. 02 (2016) 060.
[90] M. J. Baker and A. Thamm, J. High Energy Phys. 10 (2018) 187.
[91] D. A. Sierra, F. Staub, and A. Vicente, Phys. Rev. D **92**, 015001 (2015).
[92] G. Belanger, C. Delaunay, and S. Westhoff, Phys. Rev. D **92**, 055021 (2015).
[93] J. Kawamura, S. Okawa, and Y. Omura, Phys. Rev. D **96**, 075041 (2017).
[94] P. Ko, T. Nomura, and H. Okada, Phys. Lett. B **772**, 547 (2017).
[95] K. Fuyuto, H.-L. Li, and J.-H. Yu, Phys. Rev. D **97**, 115003 (2018).
[96] J. M. Cline, Phys. Rev. D **97**, 015013 (2018).
[97] J. M. Cline and J. M. Cornell, Phys. Lett. B **782**, 232 (2018).
[98] A. Azatov, D. Barducci, D. Ghosh, D. Marzocca, and L. Ubaldi, J. High Energy Phys. 10 (2018) 092.
[99] P. Rocha-Moran and A. Vicente, Phys. Rev. D **99**, 035016 (2019).
[100] N. Bernal, D. Restrepo, C. Yaguna, and Ó. Zapata, Phys. Rev. D **99**, 015038 (2019).
[101] L. Darme, K. Kowalska, L. Roszkowski, and E. M. Sessolo, J. High Energy Phys. 10 (2018) 052.
[102] S.-M. Choi, Y.-J. Kang, H. M. Lee, and T.-G. Ro, J. High Energy Phys. 10 (2018) 104.
[103] G. Kumar, C. Hati, J. Orloff, and A. M. Teixeira, in *16th Conference on Flavor Physics and CP Violation (FPCP 2018) Hyderabad, India* (Springer, Cham, 2018), Vol. 234, p. 417.
[104] S. Singirala, S. Sahoo, and R. Mohanta, Phys. Rev. D **99**, 035042 (2019).
[105] C. Hati, G. Kumar, J. Orloff, and A. M. Teixeira, J. High Energy Phys. 11 (2018) 011.
[106] A. Falkowski, S. F. King, E. Perdomo, and M. Pierre, J. High Energy Phys. 08 (2018) 061.
[107] N. Okada, S. Okada, and D. Raut, Phys. Rev. D **100**, 035022 (2019).
[108] S. Baek and C. Yu, J. High Energy Phys. 11 (2018) 054.
[109] P. T. P. Hutauruk, T. Nomura, H. Okada, and Y. Orikasa, Phys. Rev. D **99**, 055041 (2019).
[110] A. Biswas and A. Shaw, J. High Energy Phys. 05 (2019) 165.
[111] D. G. Cerdeno, A. Cheek, P. Martin-Ramiro, and J. M. Moreno, Eur. Phys. J. C **79**, 517 (2019).
[112] S. Baek, J. High Energy Phys. 05 (2019) 104.
[113] R. Barbier *et al.*, Phys. Rep. **420**, 1 (2005).
[114] C. Brust, A. Katz, S. Lawrence, and R. Sundrum, J. High Energy Phys. 03 (2012) 103.
[115] C. Smith in *Proceedings, 34th International Conference on High Energy Physics (ICHEP 2008), Philadelphia, Pennsylvania, 2008*.
[116] C. Csaki, Y. Grossman, and B. Heidenreich, Phys. Rev. D **85**, 095009 (2012).
[117] M. Papucci, J. T. Ruderman, and A. Weiler, J. High Energy Phys. 09 (2012) 035.
[118] C. Autermann, Prog. Part. Nucl. Phys. **90**, 125 (2016).
[119] A. Strumia, J. High Energy Phys. 04 (2011) 073.
[120] E. Hardy, J. High Energy Phys. 10 (2013) 133.
[121] A. Arvanitaki, M. Baryakhtar, X. Huang, K. van Tilburg, and G. Villadoro, J. High Energy Phys. 03 (2014) 022.
[122] M. R. Buckley, D. Feld, S. Macaluso, A. Monteux, and D. Shih, J. High Energy Phys. 08 (2017) 115.

[123] M. Escudero, A. Berlin, D. Hooper, and M.-X. Lin, J. Cosmol. Astropart. Phys. 12 (2016) 029.
[124] G. F. Giudice and A. Masiero, Phys. Lett. B **206**, 480 (1988).
[125] G. Bhattacharyya, Phys. Rev. D **57**, 3944 (1998).
[126] R. Barbieri and F. Senia, Eur. Phys. J. C **75**, 602 (2015).
[127] H. Georgi and C. Jarlskog, Phys. Lett. **86B**, 297 (1979).
[128] R. Barbieri, L. J. Hall, S. Raby, and A. Romanino, Nucl. Phys. **B493**, 3 (1997).
[129] B. Bajc and L. Di Luzio, J. High Energy Phys. 07 (2015) 123.
[130] J. Grygier *et al.* (Belle Collaboration), Phys. Rev. D **96**, 091101 (2017); **97**, 099902(A) (2018).
[131] M. Bona *et al.* (UTfit Collaboration), J. High Energy Phys. 03 (2008) 049.
[132] Y. Amhis *et al.* (Heavy Flavor Averaging Group (HFAG)), arXiv:1412.7515.
[133] C. Patrignani *et al.* (Particle Data Group). Chin. Phys. C **40**, 100001 (2016).
[134] A. Pich, Prog. Part. Nucl. Phys. **75**, 41 (2014).
[135] J. Brod, M. Gorbahn, and E. Stamou, Phys. Rev. D **83**, 034030 (2011).
[136] R.-M. Wang, Y.-G. Xu, M.-L. Liu, and B.-Z. Li, J. High Energy Phys. 12 (2010) 034.
[137] F. Feruglio, P. Paradisi, and A. Pattori, Phys. Rev. Lett. **118**, 011801 (2017).
[138] F. Feruglio, P. Paradisi, and A. Pattori, J. High Energy Phys. 09 (2017) 061.
[139] Y. Kao and T. Takeuchi, arXiv:0910.4980.
[140] A. de Gouvea, S. Lola, and K. Tobe, Phys. Rev. D **63**, 035004 (2001).
[141] S. Esch, M. Klasen, D. R. Lamprea, and C. E. Yaguna, Eur. Phys. J. C **78**, 88 (2018).
[142] T. Banks, J.-F. Fortin, and S. Thomas, arXiv:1007.5515.
[143] E. Aprile *et al.* (XENON Collaboration), Phys. Rev. Lett. **121**, 111302 (2018).
[144] B. J. Kavanagh, P. Panci, and R. Ziegler, J. High Energy Phys. 04 (2019) 089.
[145] A. Greljo, J. M. Camalich, and J. D. Ruiz-Alvarez, Phys. Rev. Lett. **122**, 131803 (2019).
[146] D. Dercks, H. Dreiner, M. E. Krauss, T. Opferkuch, and A. Reinert, Eur. Phys. J. C **77**, 856 (2017).
[147] A. Chakraborty and S. Chakraborty, Phys. Rev. D **93**, 075035 (2016).
[148] B. M. Dassinger, T. Feldmann, T. Mannel, and S. Turczyk, J. High Energy Phys. 10 (2007) 039.